A Variable Structure Controller for a Single Stage Three Level Resonant PFC Rectifier

Mohammed S. Agamy, *Student member IEEE* and Praveen K. Jain, *Fellow IEEE*
Energy and Power Electronics Applied Research Laboratory (*e*PEARL)
Department of Electrical and Computer Engineering
Queen's University
Kingston, ON, K7L 3N6 Canada

***Abstract*- This paper presents a variable structure control method for a single stage three level resonant AC/DC converter. A switching functions to regulate both the input current and dc-bus voltage. This controller also makes the system response less sensitive to load variations, supply voltage changes and resonant tank parameter variations.**

I. INTRODUCTION

The power handling capability and component stresses of single-stage power factor corrected converters have always set severe restrictions on their applicability to low power circuits. In order to reduce component stresses for the different converter operating conditions, three level topologies can be employed [1]. Therefore, by combining the features of boost power factor pre-regulators, resonant converters and three-level dc/dc topologies, a single stage three level half bridge series parallel resonant AC/DC converters with a current shaping input inductor that can provide an efficient, high power density, low component stresses solution for front end telecommunications power supplies that can operate at higher power levels and universal input voltage range (90-265Vrms) is obtained. The control of this converter is achieved by a combined variable frequency and asymmetrical pulse width modulation control. Variable frequency is used to tightly regulate the output voltage and APWM control is for current shaping and to control the dc-bus voltage under all loading conditions. The converter can operate with either continuous or discontinuous input current. The continuous conduction mode operation is preferable as it reduces the electromagnetic interference resulting from the converter operation as well as obtaining a high efficiency, which is important for the higher power levels the converter is designed to operate under (multiple kilowatts). On the other hand, continuous conduction mode requires three feedback signals: the output voltage, input current and the dc-bus voltage. Another critical aspect for controlling resonant converters is the parameter tolerances which can degrade the circuit operation if not fully anticipated in the controller design [2].

Sliding mode control is a simple and effective method for controlling non-linear systems, including power electronic converters. This controller has the advantages of fast response as well as making the system response less sensitive to load variations, supply voltage changes and circuit parameter variations. This makes it suitable to apply this control technique to universal input voltage levels. Sliding mode control is also seen suitable for this kind of applications because power converters inherently have multiple structures according to the state of switch(es) [3-5].

In this paper a sliding mode control method is presented for a three level resonant half bridge circuit operating as a single stage power factor correction converter, operating with continuous or discontinuous input current. The sliding mode controller replaces both the outer and inner control loops needed for dc-bus voltage regulation and input current shaping, as they are both replaced by one switching function.

II. POWER CIRCUITS

The proposed circuit, shown in figure 1, is composed of a series parallel LCC three level resonant circuit with an input boost inductor directly connected to the lower pair of the converter switches. The boost inductor L_{in} operates in either discontinuous conduction mode (DCM) or continuous conduction mode (CCM). The control of this converter is achieved via a combined APWM and Variable frequency controller. The duty cycle obtained from the APWM controller serves to regulate the DC-bus voltage foe all input and output conditions, whereas the variable frequency controller gives a tightly regulated output voltage. A simplified block diagram of the closed loop operation and a timing diagram are shown in figure 2 and figure 3.

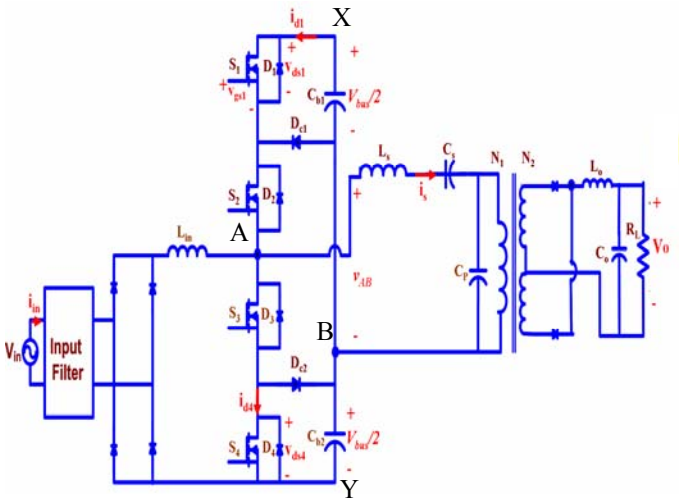

Figure 1 Topology of 3-level SSPFC Converter

978-1-4244-1874-9/08/$25.00 ©2008 IEEE

In this circuit, the upper and lower pairs of switches operate complimentarily. When S_3 and S_4 are ON energy from the supply is stored in the boost inductor (L_{in}) while the bulk capacitor (C_{b2}) supplies energy to the load through the resonant circuit. Therefore, the voltage across the resonant circuit during this period is ($-V_2$). Switch S_4 is made to turn off a very short time before S_3 to allow the voltage across S_4 to be clamped to (V_2) through clamping diode D_{c2}. This stage of operation ends at $t=d_1T_s$, where d_1 is the duty cycle of the boost stage and T_s is the switching period. The following stage occurs when switches S_1 and S_2 are in the ON state. During this period the input inductor discharges its energy into the bulk capacitors C_{b1} and C_{b2} in series, whereas, C_{b1} is responsible for supplying energy to the output load through the resonant circuit. The duration of this period is d_2T_s. Finally, the current of the resonant inductor reaches zero and the operation of the circuit continues as the bulk capacitor C_{b1} supplies energy to the output load. This goes on for the remaining part of the switching cycle d_3T_s. Due to the asymmetry of the waveform of the input voltage to the resonant circuit (v_{AB}) the resonant circuit must contain a series capacitor C_s to block the dc component of the input voltage and avoid transformer saturation.

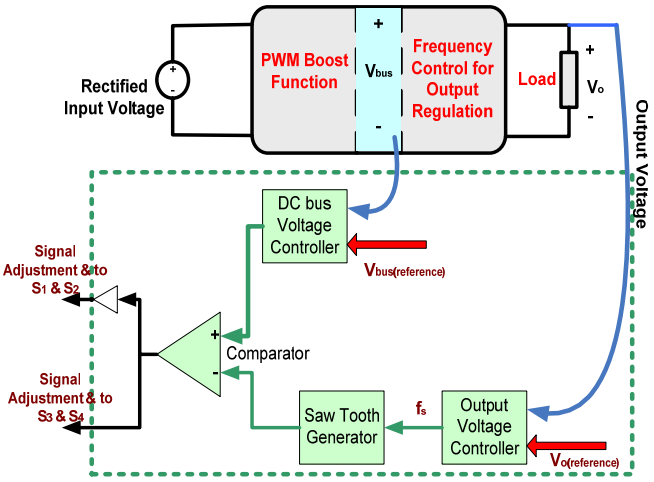

Figure 2 Simplified block diagram of the closed loop system

III. Mathematical Model

Due to the use of two control variables: frequency and pulse width, the converter model should be able to separate both control variables so that controller design would be more simple and accurate. Therefore, a combined averaging and multiple frequency modeling approach is used to represent the converter dynamics [6,7].

For continuous conduction mode, considering the two operating conditions per switching cycle shown in figure 4, The operation of the converter can be divided into two main periods: (i) when lower switches (S_3 & S_4) are on, $0 \le t \le DT_s$ and (ii) when upper switches (S_1 & S_2) are on, $DT_s \le t \le T_s$ and the average model per switching cycle can be given by:

$$\frac{d}{dt}\begin{bmatrix} i_{Lin} \\ V_1 \\ V_2 \\ i_s \\ v_s \\ v_P \end{bmatrix} = \begin{bmatrix} 0 & -\frac{(1-D)}{L_{in}} & -\frac{(1-D)}{L_{in}} & 0 & 0 & 0 \\ \frac{(1-D)}{C_{b1}} & 0 & 0 & -\frac{(1-D)}{C_{b1}} & 0 & 0 \\ \frac{(1-D)}{C_{b2}} & 0 & 0 & \frac{D}{C_{b2}} & 0 & 0 \\ 0 & \frac{D}{L_s} & \frac{-(1-D)}{L_s} & 0 & \frac{-1}{L_s} & \frac{-1}{L_s} \\ 0 & 0 & 0 & \frac{1}{C_s} & 0 & 0 \\ 0 & 0 & 0 & \frac{1}{C_P} & 0 & \frac{-1}{C_P R_{ac}} \end{bmatrix} \begin{bmatrix} i_{Lin} \\ V_1 \\ V_2 \\ i_s \\ v_s \\ v_P \end{bmatrix} + \begin{bmatrix} \frac{1}{L_{in}} \\ 0 \\ 0 \\ 0 \\ 0 \\ 0 \end{bmatrix} |v_{in}| \quad \ldots\ldots (1)$$

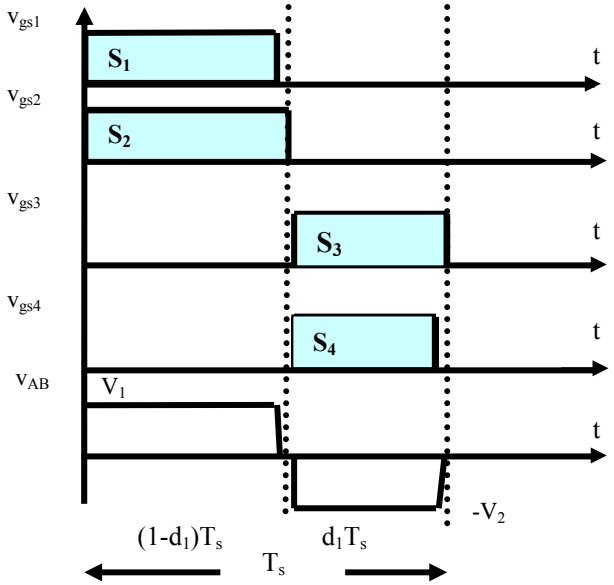

Figure 3 Switching sequence

All state variable notations are defined on the circuit diagram in figure 4 and

$$R_{ac} = \frac{\pi^2}{8}\left(\frac{N_1}{N_2}\right)^2 R_L \quad \ldots\ldots (2)$$

For discontinuous conduction mode, the major stages of operation are shown in figure 5. The basic operation of the converter can be divided into three parts: Switches S_3 and S_4 are ON, this occurs in the interval $0 \le t \le DT_s$, where T_s is the switching period and $d_1<1$ is the fraction of the period during which this operation occurs. The second set of dynamic equations occurs when switches S_1 and S_2 are ON with the input inductor discharging its energy. This occurs during the time period $DT_s \le t \le (D+d_2)T_s$. The third stage takes place with switches S_1 and S_2 still in the ON state. The duration of this period is d_3T_s. The average model over one switching period is thus, given by:

$$[\dot{x}] = A_{eq}[x] + B_{eq}|v_{in}| \quad \ldots\ldots (3)$$

Such that,

$$[x] = [i_{Lin} \quad V_1 \quad V_2 \quad i_s \quad v_s \quad v_p]^t \quad \ldots\ldots (4)$$

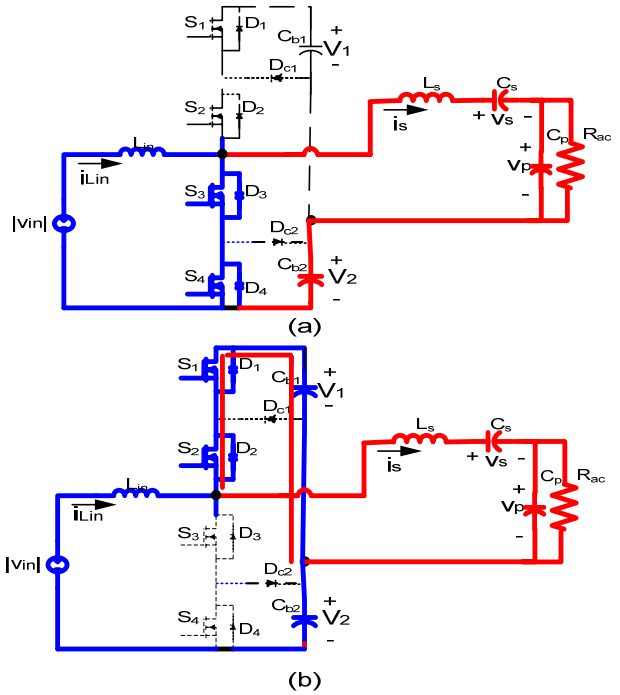

Figure 4 Equivalent Circuits for the two stages of operations in CCM (a) input inductor charging, (b) input inductor discharging

is the state vector,

$$A_{eq}=\begin{bmatrix} 0 & -\frac{d_2}{L_{in}} & -\frac{d_2}{L_{in}} & 0 & 0 & 0 \\ \frac{d_2}{C_{b1}} & 0 & 0 & -\frac{(1-D)}{C_{b1}} & 0 & 0 \\ \frac{d_2}{C_{b2}} & 0 & 0 & \frac{D}{C_{b2}} & 0 & 0 \\ 0 & \frac{(1-D)}{L_s} & -\frac{D}{L_s} & 0 & -\frac{1}{L_s} & -\frac{1}{L_s} \\ 0 & 0 & 0 & \frac{1}{C_s} & 0 & 0 \\ 0 & 0 & 0 & \frac{1}{C_p} & 0 & -\frac{1}{R_{ac}C_p} \end{bmatrix} \quad \ldots\ldots (5)$$

is the plant matrix,

$$B_{eq}=\left[\frac{(D+d_2)}{L_{in}} \quad 0 \quad 0 \quad 0 \quad 0 \quad 0\right]^t \quad \ldots\ldots (6)$$

The variable D represents the fraction of the duty cycle during which the lower pair of switches is turned ON, which is the charging period of the input inductor, i.e. D is the duty cycle of the APWM controller.

The second step of the modeling process is to express all the state variables in terms of its harmonic components. This enables obtaining the high and low frequency dynamics in the same model, in addition to that, the switching frequency can be separated as an independent control variable and the state variables will be changed into variables that have a dc-steady state value instead of having two sets of variables at two different frequency ranges. The original state variables can thus be broken down as shown in equations (7)-(10). The relationship between the two variables D and d_2 for DCM can be obtained from the current waveform as shown in figure 6 The rectified input voltage can thus be given as:

$$|v_{in}|=\frac{2V_m}{\pi}+\sum_{n=2,4,6,\ldots}\frac{4V_m}{\pi}\frac{n}{n^2-1}\cos(n\omega_l t) \quad \ldots\ldots (7)$$

where n is the harmonic order.

Similarly,

$$v_P\,\mathrm{sgn}(v_P)=|v_p|=\frac{2v_{p(\max)}}{\pi}+\sum_{n=2,4,6,\ldots}\frac{4v_{P(\max)}}{\pi}\frac{n}{n^2-1}\cos(n\omega_s t) \quad \ldots\ldots (8)$$

on the output rectifier side

The input voltage to the resonant circuit (v_{AB}) in terms of V_1 and V_2 and referring to figure 3 can be given as:

$$v_{AB}\approx V_1(1-D)-V_2D+\frac{V_1+V_2}{\pi}\sin(2\pi(1-D))\cos\omega_s t + \frac{V_1+V_2}{\pi}[1-\cos(2\pi(1-D))]\sin\omega_s t+\ldots \quad \ldots\ldots (9)$$

$$\left.\begin{aligned} i_s &= i_{s(dc)}+i_{sq}\cos\omega_s t+i_{sd}\sin\omega_s t \\ v_s &= v_{s(dc)}+v_{sq}\cos\omega_s t+v_{sd}\sin\omega_s t \\ v_P &= v_{P(dc)}+v_{Pq}\cos\omega_s t+v_{Pd}\sin\omega_s t \\ V_1 &= V_{1(dc)}+V_{1ql}\cos 2\omega_l t+V_{1dl}\sin 2\omega_l t \\ &\quad +V_{1q}\cos\omega_s t+V_{1d}\sin\omega_s t \\ V_2 &= V_{2(dc)}+V_{2ql}\cos 2\omega_l t+V_{2dl}\sin 2\omega_l t \\ &\quad +V_{2q}\cos\omega_s t+V_{2d}\sin\omega_s t \\ i_{Lin} &= i_{Lin(dc)}+i_{Linql}\cos 2\omega_l t+i_{Lindl}\sin 2\omega_l t \\ &\quad +i_{Linq}\cos\omega_s t+i_{Lind}\sin\omega_s t \end{aligned}\right\} \quad \ldots\ldots (10)$$

The effect of higher harmonics is very small and can, therefore, be neglected here. By substituting equations (7)-(10) in (3) and equating harmonic components taking into consideration the average power balance between input and output we can reformulate the model in (3) in terms of duty cycle and switching frequency as explicit control inputs. In order to obtain a linearized model of the converter, the two ratios D and d_2 must be replaced by a single value or at least one of them be expressed in terms of the other. Figure 6 shows the input inductor current over one switching period.

Due to the difference in dynamic response between the resonant tank and input to dc-bus section; the former being much faster in dynamic response as compared to the latter; a decoupled model can be obtained. This is achieved by considering the input to the high frequency resonant stage as a rectangular wave voltage source whose magnitude is determined by the value of the dc bus voltage. In case of fundamental analysis this would be a sinusoidal voltage source whose magnitude depends on V_{bus}. Whereas, the low

frequency current shaping boost operation can be separated as having a dc load at the output determine by the output of the converter that would have an equivalent resistance R_{eq}. A simplified schematic diagram of this separation is shown in figure 7.

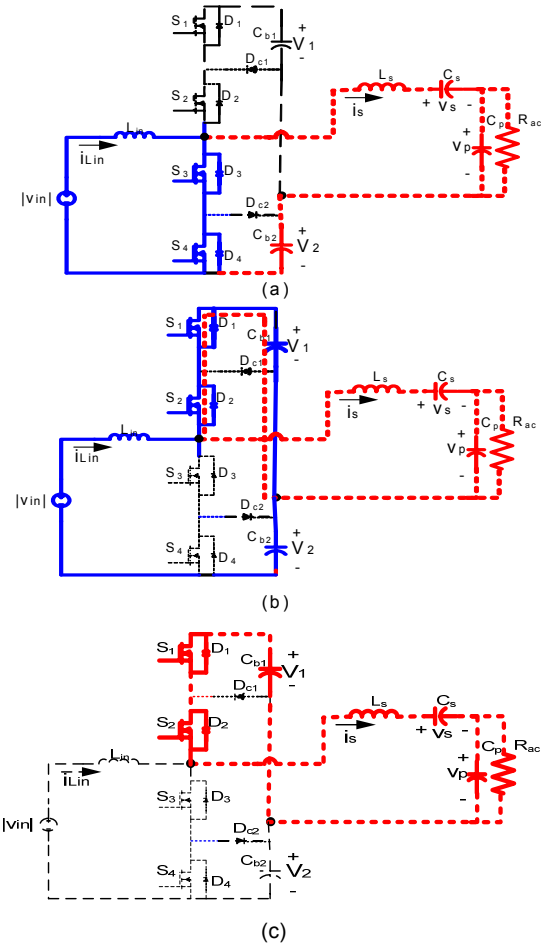

Figure 5 Equivalent Circuits for the three stages of operation DCM) (a) input inductor charging, (b) input inductor discharging, (c) Energy transfer to output

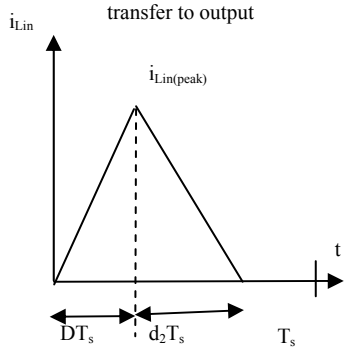

Figure 6 Input inductor current in discontinuous conduction mode

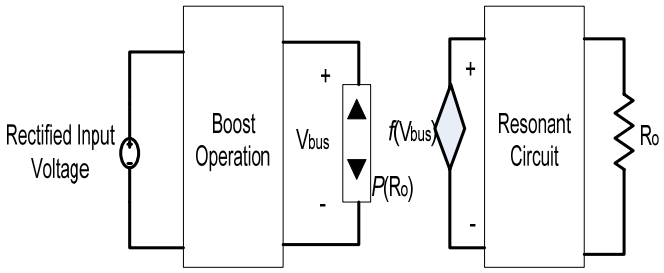

Figure 7 Simplified block diagram of the decoupled circuit

IV. Sliding Mode Controller Design

Since the converter model can be decoupled into two subsystems one for the output and one for input current shaping, the output voltage is regulated by variable frequency determined through a PI regulator of the output voltage error; this regulator has a transfer function:

$$G_{v_o} = \frac{f_s}{e_{v_o}} = \frac{2000 + 0.25s}{s} \qquad \text{.....(11)}$$

where, fs is the switching frequency, evo is the output voltage error and s is the Laplace domain variable. As for the input to dc-bus stage, a sliding mode controller will be designed to integrate both voltage and current loops. For this purpose, and since in a decoupled model the high frequency components have a much lower effect, the model of the low frequency variables can be given as:

$$\frac{d}{dt}\begin{bmatrix} i_{Lin} \\ V_1 \\ V_2 \end{bmatrix} = \begin{bmatrix} 0 & \frac{u-1}{L_{in}} & \frac{u-1}{L_{in}} \\ \frac{u-1}{C_{b1}} & \frac{-1}{R_{eq1}C_{b1}} & 0 \\ \frac{u-1}{C_{b2}} & 0 & \frac{-1}{R_{eq2}C_{b2}} \end{bmatrix} \begin{bmatrix} i_{Lin} \\ V_1 \\ V_2 \end{bmatrix} + \begin{bmatrix} \frac{1}{L_{in}} \\ 0 \\ 0 \end{bmatrix} |v_{in}| \qquad \text{.....(12)}$$

where, (u) is a variable that depends on the state of the switches (S3 and S4), such that:

$$u = \begin{cases} 1 & when \quad S_3 \ and \quad S_4 \ are \quad ON \\ 0 & when \quad S_3 \ and \quad S_4 \ are \quad OFF \end{cases} \qquad (13)$$

R_{eq1} and R_{eq2} are the equivalent resistances that ensure power flow balance through the dc-bus capacitors C_{b1} and C_{b2} respectively. For DCM equation (12) can be modified to:

$$\frac{d}{dt}\begin{bmatrix} i_{Lin} \\ V_1 \\ V_2 \end{bmatrix} = \begin{bmatrix} 0 & \left(\frac{1-\text{sgn}(v_{in})}{2}\right)\frac{u-1}{L_{in}} & \left(\frac{1-\text{sgn}(v_{in})}{2}\right)\frac{u-1}{L_{in}} \\ \frac{u-1}{C_{b1}} & \frac{-1}{R_{eq1}C_{b1}} & 0 \\ \frac{u-1}{C_{b2}} & 0 & \frac{-1}{R_{eq2}C_{b2}} \end{bmatrix}\begin{bmatrix} i_{Lin} \\ V_1 \\ V_2 \end{bmatrix} + \begin{bmatrix} \frac{1}{L_{in}} \\ 0 \\ 0 \end{bmatrix}|v_{in}| \quad \text{.....(14)}$$

Therefore, a switching surface can be given by:

$$s = g_i e_i + g_v e_{vbus} \tag{15}$$

$$u = \begin{cases} 1 & s < 0 \\ 0 & s > 0 \end{cases} \tag{16}$$

where, g_i and g_v are switching function gains, e_i and e_{vbus} are the errors of the input current and the dc-bus voltage respectively such that:

$$e_i = i_{ref} - i_{Lin},\ e_{vbus} = V_{ref} - (V_1 + V_2) \tag{16}$$

The reference output voltage is a constant DC value, whereas the reference current i_{ref} takes the waveform of a rectified sinusoid in phase with the rectified input voltage. The amplitude of this sinusoid is determined such that power flow is balanced [8]. Since the line frequency is much lower than the switching frequency, the reference values can be considered at steady state during each switching cycle.

The next step is to determine the stability of the controller. A sufficient condition for stability can be given by:

$$s\dot{s} < 0 \tag{17}$$

When $s > 0 \Rightarrow u = 0 \ \therefore \dot{s} < 0$

$$\therefore \frac{g_i}{g_v} > L_{in}\left(\frac{\frac{V_1 + i_{Lin}R_{eq1}}{R_{eq1}C_{b1}} + \frac{V_2 + i_{Lin}R_{eq2}}{R_{eq2}C_{b2}}}{|v_{in}| - V_1 - V_2}\right) \tag{18}$$

When $s < 0 \Rightarrow u = 1 \ \therefore \dot{s} > 0$

$$\therefore \frac{g_i}{g_v} < \frac{L_{in}}{|v_{in}|}\left(\frac{V_1 R_{eq2}C_{b2} + V_2 R_{eq1}C_{b1}}{R_{eq1}C_{b1}R_{eq2}C_{b2}}\right) \tag{19}$$

Req1 and Req2 are the equivalent resistances that ensure power flow balance through the dc-bus capacitors Cb1 and Cb2 respectively and

$$V_1 = \sqrt{V_{1(dc)}^2 + V_{1ql}^2 + V_{1dl}^2 + V_{1q}^2 + V_{1d}^2} \tag{20}$$

$$V_2 = \sqrt{V_{2(dc)}^2 + V_{2ql}^2 + V_{2dl}^2 + V_{2q}^2 + V_{2d}^2} \tag{21}$$

As long as (18) and (19) are satisfied the sliding condition will be satisfied and the system trajectory will move along the designed sliding surface. Consequently the equivalent duty ratio needed during each duty cycle can be calculated.

V. Input Current Observer

A state observer can be designed to estimate the input inductor current, in order to reduce the number of measurements and consequently increase the system reliability [8]. The observer dynamics can be given by:

$$\dot{z} = Az + Bu + F + K(y - Cz) \tag{22}$$

where, z represents the vector of estimated states, $z = \begin{bmatrix} \hat{i}_{Lin} & \hat{V}_1 & \hat{V}_2 \end{bmatrix}$, A, B and F are obtained by the separation of the plant matrix in (12), K is the observer parameter vector, y is the output and Cz is the output due to estimated states. In this case the only output is V_1+V_2, therefore, C= [0 1 1].

Matrix B depends on both the converter parameters and the state values. Therefore, it can be separated into a parameter matrix B' multiplied by the observed states vector z, and thus (22) can be rewritten as:

$$\dot{z} = (A + B'u)z + F + K(y - Cz) \tag{23}$$

such that,

$$A = \begin{bmatrix} 0 & \frac{-1}{L_{in}} & \frac{-1}{L_{in}} \\ \frac{-1}{C_{b1}} & \frac{-1}{R_{eq1}C_{b1}} & 0 \\ \frac{-1}{C_{b2}} & 0 & \frac{-1}{R_{eq1}C_{b1}} \end{bmatrix},\ B = \begin{bmatrix} 0 & \frac{1}{L_{in}} & \frac{1}{L_{in}} \\ \frac{1}{C_{b1}} & 0 & 0 \\ \frac{1}{C_{b2}} & 0 & 0 \end{bmatrix}$$

and $K = [K_1 \quad K_2 \quad K_3]^t$

Subtracting (15*) from (5) the error dynamics of the system would reduce to: $\dot{e} = [A + B'u + KC]e = A_{obs}e$ (24)

where, e is the estimation error vector $e = \begin{bmatrix} i_{Lin} - \hat{i}_{Lin} & V_1 - \hat{V}_1 & V_2 - \hat{V}_2 \end{bmatrix}^t$. Based on the equivalent continuous control signal of the variable structure controller (u_{eq}), the system is observable; therefore, the observer gain vector K= $[K_1\ K_2\ K_3]^t$ is designed by solving the characteristic equation:

$$|sI - A_{obs}| = 0 \tag{25}$$

Combining the state observer with the previously designed controller the conditions of existence of sliding mode will be modified to be: For $s > 0 \Rightarrow u = 0 \ \therefore \dot{s} < 0$

$$\therefore \frac{g_i}{g_v} > L_{in}\left(\frac{\frac{V_1 + i_{Lin}R_{eq1}}{R_{eq1}C_{b1}} - K_2(V_1+V_2) + \frac{V_2 + i_{Lin}R_{eq2}}{R_{eq2}C_{b2}} - K_3(V_1+V_2)}{|v_{in}| - V_1 - V_2 + K_1 L_{in}(V_1+V_2)}\right) \quad (26)$$

And for $s<0 \Rightarrow u=1 \ \therefore \dot{s}>0$

$$\therefore \frac{g_i}{g_v} < \frac{L_{in}\left(\frac{V_1 R_{eq2}C_{b2} + V_2 R_{eq1}C_{b1}}{R_{eq1}C_{b1}R_{eq2}C_{b2}} - K_2(V_1+V_2) - K_3(V_1+V_2)\right)}{|v_{in}| + K_1 L_{in}(V_1+V_2)} \quad (27)$$

Therefore, the observer parameter vector should be designed to achieved the desired error dynamics as well as to satisfy the conditions in (26) and (27).

VI. Controller Performance

The aforementioned analysis was applied to a three level LCC resonant AC/DC Converter operated under a combined variable frequency and pulse width modulation control with the following parameters : output power: 2.3kW, 48Vdc output voltage, 90-265Vrms input voltage , The dc-bus voltage is set to a range of 400 to 650 Volts corresponding to a 90-265Vrms input voltage, i.e.

$$V_{bus} = 1.03V_m + 269.3 \quad (28)$$

Figures 8 and 9 show input current an output voltage response to a 50% step load change. Figures 10 and 11 show the input voltage and current and the resonant tank voltage and current illustrating zero voltage switching respectively.

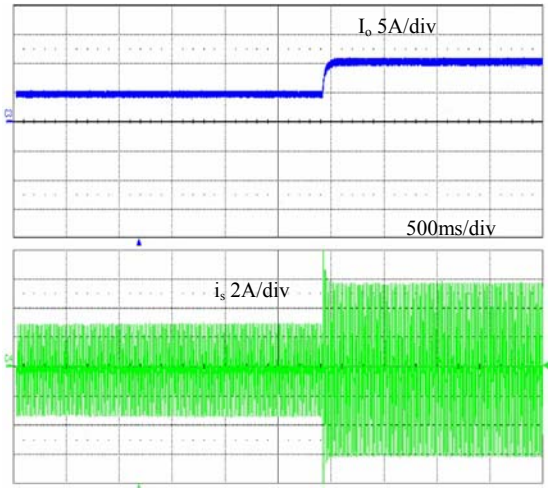

Figure 8 Experimental results: Input current with 50% step load change

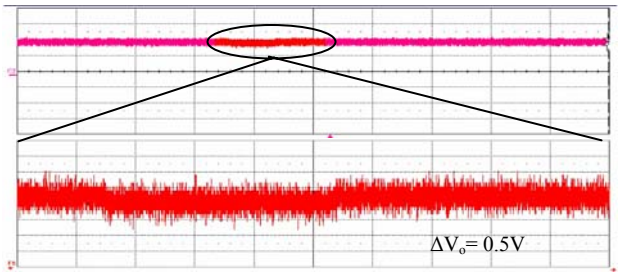

Figure 9 Output voltage response to 50% loading step

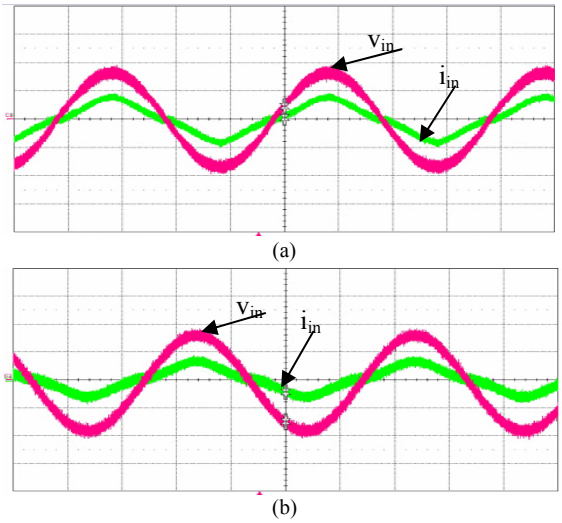

Figure 10 Input voltage and current
(a) at minimum input voltage (b) at maximum input voltage

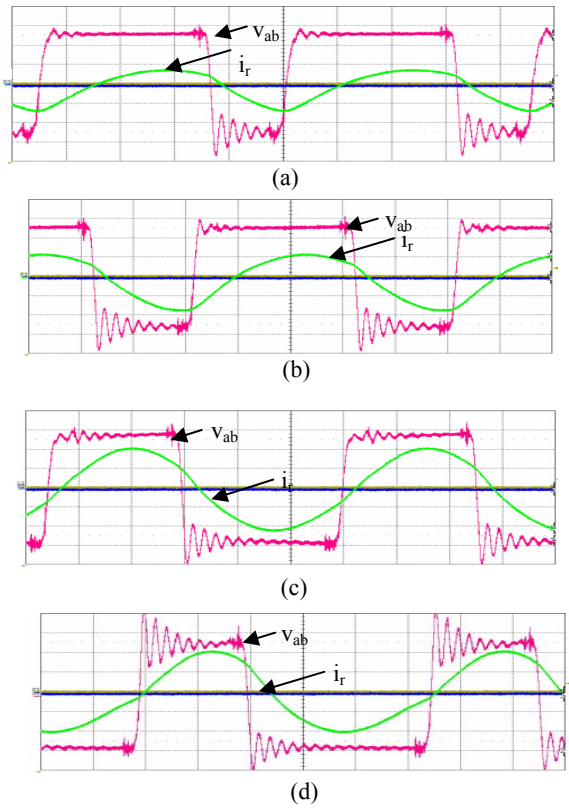

Figure 11 Resonant tank voltage (v_{ab}) and current (i_r) to illustrate lagging resonant current at different conditions figures from (a) to (d) are for increased effective loading (Higher D and lower f_s)

VII. Conclusion

A variable structure controller was proposed to control both the dc-bus voltage and input current waveform for a three-level SSPFC converter. Both perfect voltage tracking and near unity power factor were achieved over a very wide

range of loading and input voltage. The sliding mode controller is robust to system parameter variations and it is also easy to implement.

REFERENCES

[1] F. Canales, P. Barbosa & F. Lee, "A High Power Density DC/DC Converter for High Power Distributed Power System", Proceedings of Power Electronics Specialists Conference (PESC) 2003, pp.11-18.

[2] M.S. Agamy and P.K. Jain "A New Single Stage Power Factor Corrected Three Level Resonant AC/DC Converter With and Without Active Current Control", Proceedings of 40th IEEE Industry Applications Society Conference (IAS), October 2005, pp. 1992-1999.

[3] R. Morici, C. Rossi and A. Tonielli, "Variable Structure Controller for AC/DC Boost Converter", IEEE Industrial Electronics Conference IECON 1994, pp. 1449-1454.

[4] V. Utkin , J. Guldner and J. Shi, " Sliding Mode Control in Electro-Mechanical Systems", Taylor & Francis 1999.

[5] L. Rossetto, G. Spiazzi, P. Tenti, B. Fabiano and C. Licitra,, "Fast-response high-quality rectifier with sliding mode control", IEEE Trans.on Power Electronics, Vol. 9, No. 2, March 1994 146 - 152

[6] M.S. Agamy and P.K. Jain, " Modeling and Dynamics of a Single-Stage Three-level Resonant AC/DC Converter Operating with Combined Variable Frequency & PWM Control", Proceedings of the 37th Power Electronics Specialists Conference, (PESC) , June 2006, pp. 1385-1390.

[7] R. Erickson, "Fundamentals of Power Electronics", Kluwer Academic Publishers, 2nd Edition, 2001.

[8] J. Lou, N. Pongratananukul, J. Abu-Qahoouq and I. Batarseh, "Time-varying Current Observer with parameter estimation for Multiphase Low Voltage High Current Voltage Regulator Modules", Applied Power Electronics Conference and Exposition(APEC), 2003, pp. 444-450.